Supporting Information for

Three-Phase Morphology Evolution in Sequentially Solution-Processed Polymer Photodetector: Towards Low Dark Current and High Photodetectivity

Hanyu Wang,[†,‡] Shen Xing,[†] Yifan Zheng,[†,‡] Jaemin Kong,[‡,§] Junsheng Yu,[,†] and André D. Taylor[*,‡,§]*

[†]State Key Laboratory of Electronic Thin Films and Integrated Devices, School of Optoelectronic Information, University of Electronic Science and Technology of China (UESTC), Chengdu 610054, P. R. China

[‡]Department of Chemical and Environmental Engineering, Yale University, New Haven, Connecticut 06511, United States

[§]Department of Chemical and Biomolecular Engineering, Tandon School of Engineering, New York University, New York, NY 11201, United States

[*]Corresponding authors. E-mail address: jsyu@uestc.edu.cn (Yu), adt4@nyu.edu (Taylor)

Photodetector characterization

For PPDs, the figures of merit which need to be evaluated include responsivity (R) and specific detectivity (D^*). R is calculated by the ratio of the photocurrent to the intensity of the incident light as Eq. S1:

$$R(\lambda) = \frac{J_{ph}}{L_{light}} = \mathrm{EQE}(\lambda)\frac{\lambda q}{hc}(\mathrm{A/W}) \tag{S1}$$

where q is the electron charge, λ is the wavelength, h is the Planck constant, c is the light velocity, and L_{light} is the incident light intensity.

D^* is used to estimate the signal-to-noise ratio of photodetectors. The D^* of PPDs is calculated using the following Eq. S2:

$$D^*(\lambda) = \frac{R(\lambda)}{\sqrt{2q \cdot J_d}}(\mathrm{Jones}) \tag{S2}$$

where q is the absolute value of electron charge (1.6×10^{-19} Coulombs). From the equation, it is obvious that the higher responsivity is desirable for lower J_{d}.

The hole-only devices with a configuration of Ag/PEDOT : PSS/Active layers/PEDOT : PSS/Ag and electron-only devices with a configuration of Mg : Ag/Active layers/Mg : Ag were fabricated, respectively. The hole mobility in the hole-only devices and the electron mobility in the electron-only devices can be calculated using Mott-Gurney law as Eq. S3.

$$J = \frac{9}{8}\varepsilon\varepsilon_0\mu\frac{V^2}{d^3} \tag{S3}$$

where ε is the relative permittivity of organic materials assumed to be 3, and ε_0 is the vacuum dielectric constant of 8.85×10^{-12} F/m. V is the voltage, and d is the thickness of active layer.

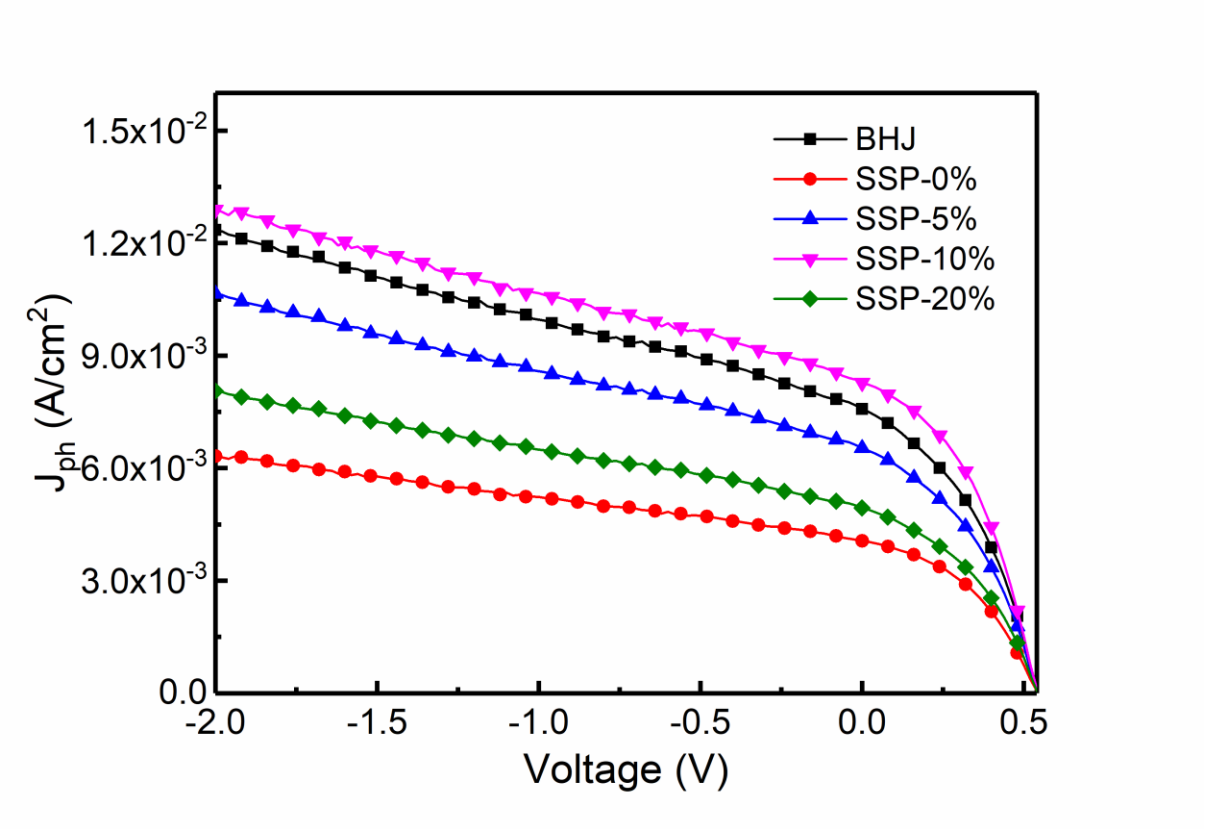

Figure S1. *J-V* characteristics of PPDs under AM 1.5 light illumination.

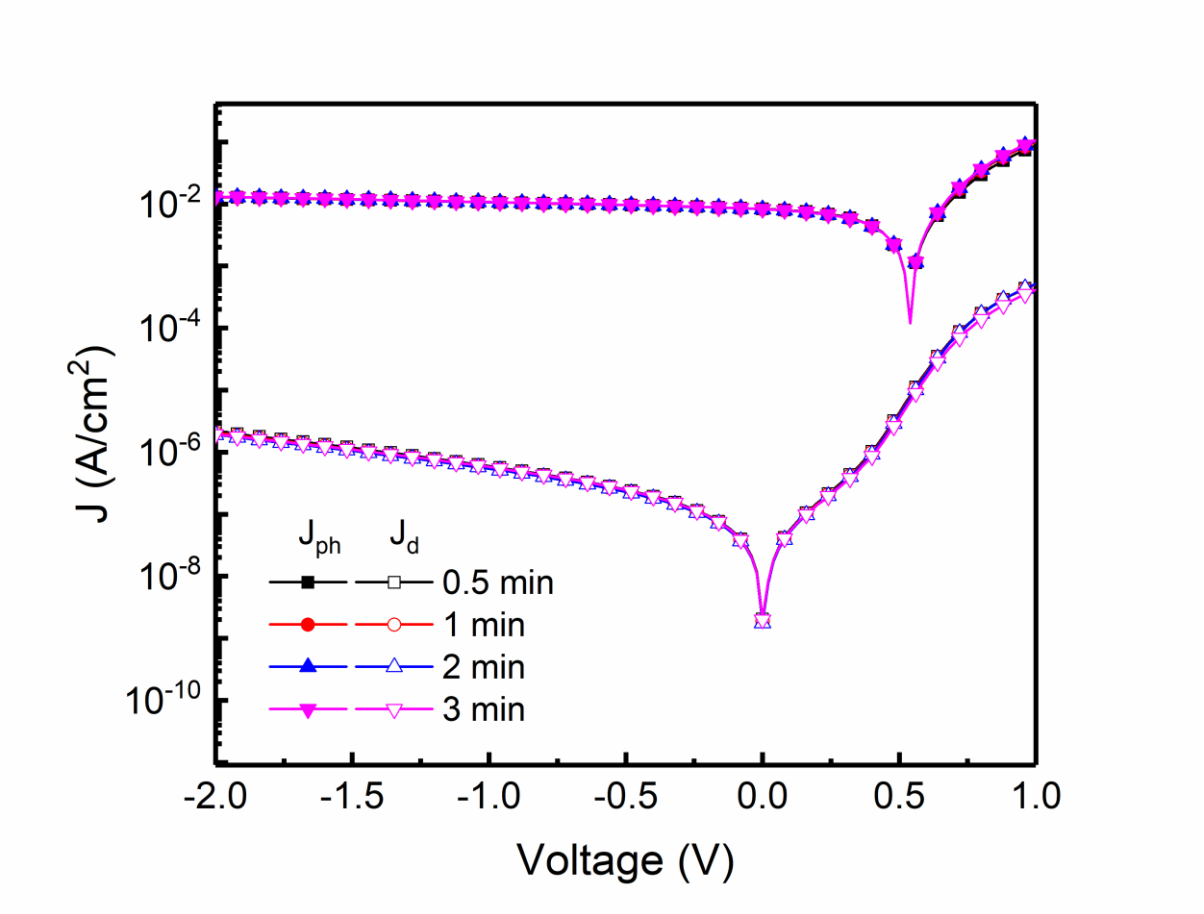

Figure S2. Semi-log *J-V* characteristics of SSP-10% PPDs with different swelling time from 0.5, 1, 2, to 3 min in dark and under AM 1.5 light illumination.

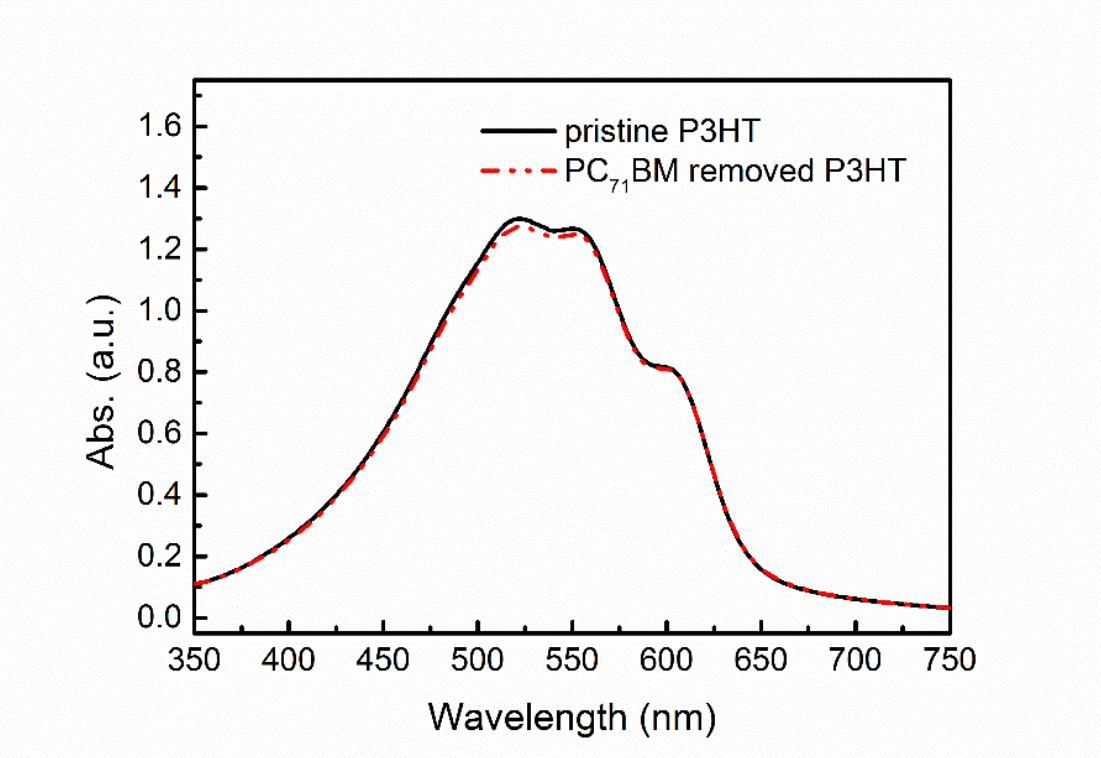

Figure S3. UV-visible absorption spectra of pristine P3HT film and an P3HT film onto which a $PC_{71}BM$ layer had been spun from 2-CP : ODCB (9 : 1) and then subsequently removed by spin coating the bilayer with 2-CP, which is marked as "$PC_{71}BM$ removed P3HT" in the inset.

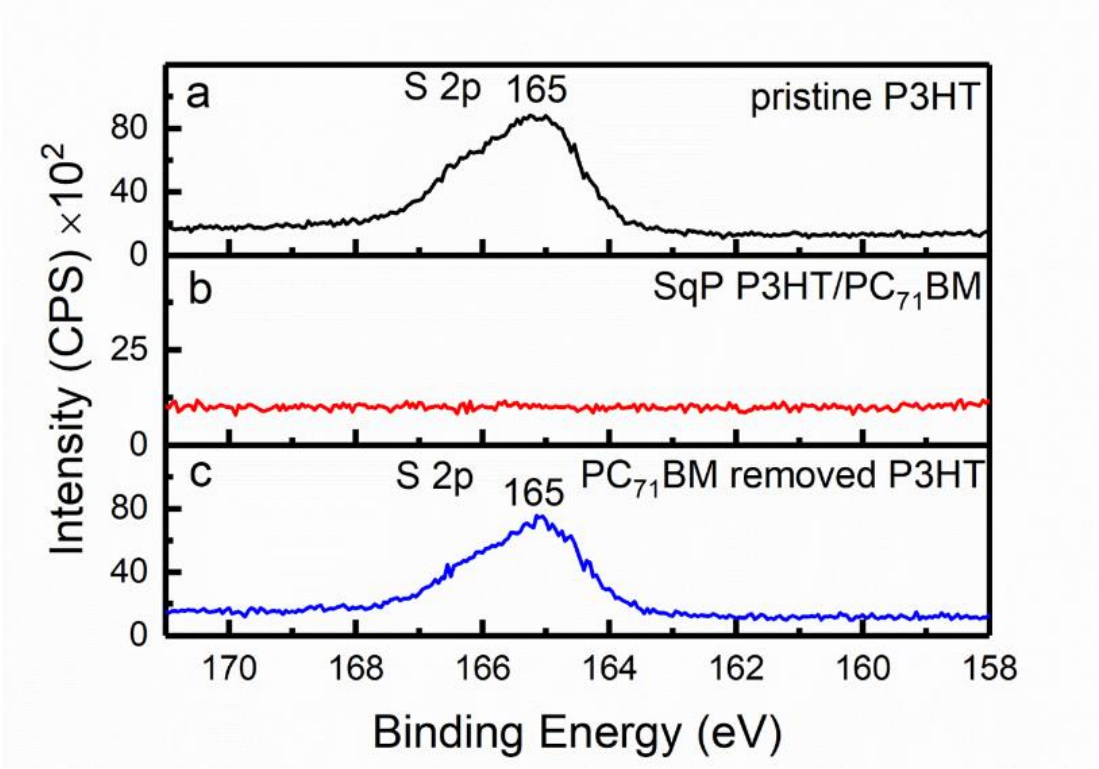

Figure S4. XPS spectra (counts per second, cps vs. binding energy, B.E.) of the S 2p peaks for (a) pristine P3HT, (b) SSP P3HT/$PC_{71}BM$, and (c) $PC_{71}BM$ removed P3HT films on silicon/silicon oxide substrates. The XPS data were taken at a take-off angle of 90° for all the films.

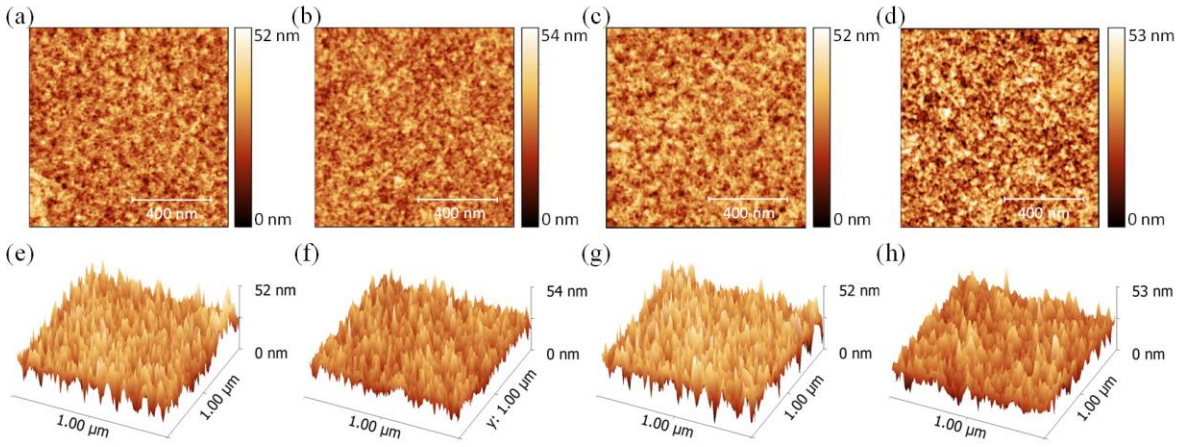

Figure S5 AFM height images (1 µm × 1 µm) of SSP-10% P3HT underlayers with different soaking times from (a) 0.5 min, (b) 1 min, (c) 2min, to (d) 3 min. The $PC_{71}BM$ layers on P3HT films were removed by spin coating 2-CP on them. The corresponding three-dimensional (3D) images are Figure e, f, g, and h.

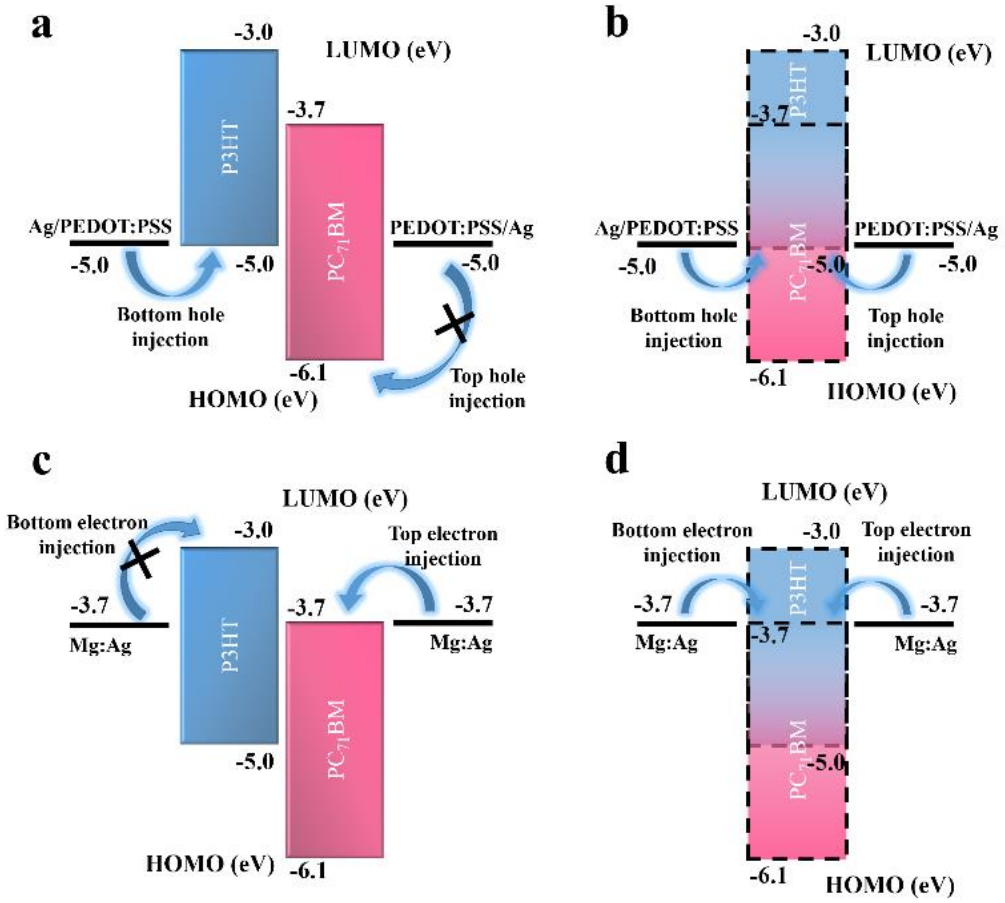

Figure S6. Schematic energy level diagrams of (a) SSP-10% hole-only device under bottom and top hole injection, (b) BHJ hole-only device under bottom and top hole injection, (c) SSP-10% electron-only device under bottom and top electron injection, and BHJ electron-only device under bottom and top electron injection.

Table S1. Photocurrent density, dark current density, and on/off current ratio of SSP-10% PPDs with different swelling time at -0.5 V.

Soaking time (min)	J_{ph} (A/cm^2)	J_d (A/cm^2)	On/off current ratio
0.5	9.65×10^{-3}	2.48×10^{-7}	3.89×10^{4}
1	9.62×10^{-3}	2.45×10^{-7}	3.93×10^{4}
2	9.65×10^{-3}	2.49×10^{-7}	3.88×10^{4}
3	9.69×10^{-3}	2.51×10^{-7}	3.86×10^{4}

Table S2. EQE of PPDs to UV, blue, green and red lights at -0.5 V.

PPD	EQE at 380 nm (%)	EQE at 470 nm (%)	EQE at 550 nm (%)	EQE at 620 nm (%)
BHJ	49.6	62.3	63.8	37.8
SSP-0%	24.5	32.0	34.8	22.9
SSP-10%	48.0	62.7	68.2	49.3

Table S3. *R* of PPDs to UV, blue, green and red lights at -0.5 V.

PPD	*R* at 380 nm (A/W)	*R* at 470 nm (A/W)	*R* at 550 nm (A/W)	*R* at 620 nm (A/W)
BHJ	0.152	0.236	0.283	0.189
SSP-0%	0.075	0.121	0.154	0.114
SSP-10%	0.147	0.238	0.302	0.246

Table S4. D^* of PPDs to UV, blue, green and red lights at -0.5 V.

PPD	D^* at 380 nm (Jones)	D^* at 470 nm (Jones)	R at 550 nm (Jones)	R at 620 nm (Jones)
BHJ	1.24×10^{11}	1.93×10^{11}	2.31×10^{11}	1.54×10^{11}
SSP-0%	3.54×10^{11}	5.73×10^{11}	7.29×10^{11}	5.40×10^{11}
SSP-10%	5.96×10^{11}	9.64×10^{11}	1.23×10^{12}	9.99×10^{11}